Eurographics Workshop on Visual Computing for Biology and Medicine (2012)
T. Ropinski, A. Ynnerman, C. Botha, and J. Roerdink (Editors)

Geometrical-Acoustics-based Ultrasound Image Simulation

Yuen C. Law, Thomas Knott, Bernd Hentschel and Torsten Kuhlen

Virtual Reality Group, RWTH Aachen University, Germany

Abstract

Brightness modulation (B-Mode) ultrasound (US) images are used to visualize internal body structures during diagnostic and invasive procedures, such as needle insertion for Regional Anesthesia. Due to patient availability and health risks—during invasive procedures—training is often limited, thus, medical training simulators become a viable solution to the problem. Simulation of ultrasound images for medical training requires not only an acceptable level of realism but also interactive rendering times in order to be effective. To address these challenges, we present a generative method for simulating B-Mode ultrasound images using surface representations of the body structures and geometrical acoustics to model sound propagation and its interaction within soft tissue. Furthermore, physical models for backscattered, reflected and transmitted energies as well as for the beam profile are used in order to improve realism. Through the proposed methodology we are able to simulate, in real-time, plausible view- and depth-dependent visual artifacts that are characteristic in B-Mode US images, achieving both, realism and interactivity.

1. Introduction

Due to its low cost and non-invasive and non-radioactive nature, ultrasound (US) is often preferred over other imaging methods such as tomography or magnetic resonance, as a tool for diagnosis. Another important use of US imaging is in the guidance of invasive procedures such as regional anesthesia and biopsies. The main issue is that US images are rather noisy and blurry and physicians require considerable experience to be able to identify organs, pathologies and other structures.

Training of US for diagnosis is generally done with real machines on patients and fellow trainees, since it is non-invasive and presents little or no risk to them. The problem of this training approach is the low availability of patients to train on specific pathologies. Some pathologies are very rare, and a trainee might need to wait a long time before encountering one. A second approach is the use of phantoms, physical devices, e.g., mannequins, with artificial substances and structures that try to mimic real body tissue and organs. These, of course, are far from real-life scenarios. Obtaining adequate training for invasive procedures, e.g., US guided needle insertion procedures, is further limited by the fact that these procedures do require to insert a needle into the patient, and when performed wrongly can indeed represent a risk for them.

Virtual Reality simulators then become a good option to obtain the desired training for various reasons; the first and probably most important is that the health of patients is not at risk during training sessions. Second, different scenarios can be created to train on a large variety of pathologies and procedures—even the ones that are uncommon. And finally, a higher level of realism over the use of phantoms can be achieved, not only with the generation of images, but also on haptic feedback and life-like scenarios as a whole. Attaining suitable simulators for training needs meeting certain requirements. For example, adequate levels of realism and detail, as well as real-time interaction, are important to enable effective training. Additionally, as already discussed, the simulator should facilitate the creation of a diversity of training scenarios and changing simulation and training parameters.

In this paper, we present a simulation approach that addresses the aforementioned challenges through different techniques. Realism is achieved by using reasonably complex physical models to estimate ultrasonic echo signals from tissues with different characteristics and by modeling ultrasound propagation through tissue using a ray-based approach. This also contributes to the parametrization of the simulation, since tissue characteristics and the input to the models can be easily changed. Real-time interaction is achieved by parallelization of the algorithms and estima-

tions. The primary contribution of this paper is the description of the used physical models and their implementation.

The rest of this paper is structured as follows. First we give a brief overview of existing approaches and related work. In section 3 we give a detailed description of the applied physical models. In section 4 we present implementation details and the results are discussed in section 5. Finally, in section 6 we discuss on the lessons learned and give an overview on future work.

2. Related Work

Ultrasound images can be simulated through different approaches. These can be classified into two major groups: *interpolative* and *generative* [GS09]. Interpolative approaches [ACO98, NCQ*11] are able to generate ultrasound images by sampling from real pre-acquired images, filling in the missing gaps, where necessary, with interpolation. These approaches are preferred when real time (RT) simulation is needed, i.e., in training simulations. A major drawback is the low availability of adequate samples to work with, thus, limiting the number of training scenarios that can be created. Acquisition from different angles is required to create the volumes since US images contain view-dependent artifacts, i.e., acoustic shadows, that might occlude part of the sampled images. As a result, the process is time-consuming. Furthermore, the acoustic shadows must be removed from the samples to generate the volumetric dataset and are therefore not included in the simulation. Additionally, depth-dependent artifacts resulting from the focusing characteristics of the US beam, such as point-spreading, might look unrealistic if the simulation viewing planes do not match the pre-acquired ones. These problems have been addressed by some authors [Zhu06, MZR*07].

In contrast, generative approaches [BD80,Jen91,KWN10] simulate sound propagation with accurate wave models and their interaction with tissue. These approaches model the complete interaction of the wave front with the medium resulting in accurate simulations that require complex calculations. Due to this complexity, generative approaches are slow, possibly taking hours to render a single image.

Another issue with generative approaches arises from the fact that some tissues are difficult to characterize in an accurate way, hence, some of the resulting textures may look artificial. In fact, a research area closely related to US image simulation is ultrasonic tissue characterization (UTC) [LN82]. Its main purpose is to extract quantitative information from US to evaluate characteristics of tissue to identify pathologies and thereby improve diagnostics [Thi03]. This is done by studying the interaction of US waves within the soft tissue and analyzing their behavior, i.e., changes in velocity, absorption, attenuation and scattering patterns [LN82].

In recent years, with the development of massively parallel GPUs, rendering times have been greatly reduced, enabling the development of more suitable training case scenarios. This resulted in hybrid approaches, which make use of generative and interpolative ideas [WBK*08, SHN08, KSN09, RPAS09]. These solutions use pre-acquired CT images as a source for tissue characterization and combine them with efficiently computable physical models to predict sound propagation and interaction within this tissue. This enables more accurate images with view- and depth-dependent artifacts to be simulated while maintaining real-time interaction. However, some of the artifacts that are commonly seen in real US images are not included in this model, e.g., mirroring and reverberation. Others, i.e., blurring and speckle patterns, are added in a somewhat artificial post-processing step, e.g., using filters and noise textures. All these artifacts are important for training scenarios since they are either used to recognize certain structures or may represent pitfalls that trainees must learn to avoid, e.g., they should be able to differentiate between a real structure and its mirror image. Furthermore, dependence on CT images for simulation still limits the number of possible training scenarios.

The generative solution that we propose uses a geometrical-acoustics approach [Vor08] to model wave propagation with rays, using physics from optics, to generate interactively simulated ultrasound images from explicit surface representations, i.e., triangle meshes, and tissue characterizations found in literature. We also borrow some results from UTC research to model the simulated tissue to produce realistic speckle patterns and reflections. With this approach, as we do not directly use information from pre-acquired images, we are able to reduce the dependence to these and to obtain different scenarios, i.e., the simulation parameters can be changed to produce different results, thus, separating tissue modeling and characterization from ultrasound simulation. Furthermore, the ray-based approach to sound propagation requires less calculation compared to the wave-based approach and although the results might not be as accurate, we will show that they are still plausible.

3. Theoretical Background

In this section, we will briefly describe the physical models involved in the actual simulation, as well as some of the basic theory behind US imaging.

3.1. Sampling and Image Formation

Typical US probes consist of an array of transducers; the quantity varies between 128 and 256. The transducers, or groups of transducers, are stimulated sequentially to send acoustic pulses into the tissue to "sweep" the area of interest and obtain the desired image. By doing so, ultrasound beams cause little or no interference to one another. After sending the pulse, the transducers are set to receive mode to wait for incoming echoes. The direction of the beam, intensity of the echoes and the time difference between sent and received

signals determine the intensity values of pixels in the final image.

During the image-formation process in common US imaging systems, two assumptions are made: (1) the ultrasound beam is perfectly focused along its axis, i.e., no side beams or variations in beam width or direction due to refraction are taken into consideration, and (2) the speed of sound has a constant value of $1540 m/s$ regardless of tissue density. Consequently, (1) detected echo signals are always displayed, in the image, along the axis of the beam, although the real position of the corresponding reflector, i.e., the object that causes the echo, might not lie on it. This affects the lateral resolution of the resulting image, causing objects to appear blurry along the x axis. And (2) the estimated distance from the transducer is not always accurate.

3.2. Beam Model

The profile of an US beam varies depending on transducer size, shape and configuration. A superposition of Gaussian beams can be used to model the amplitude variations of the ultrasound wave according to distance and direction from the transducer [WB88]. By changing the parameters of the transducer model, e.g., radius, frequency, and focal length, different beam profiles can be simulated. It is also possible to change the number of Gaussian beams and their coefficients to simulate different types of transducers.

3.3. Sound Propagation

In geometrical acoustics [Vor08], the behavior of the sound wave is approximated with energy-transporting rays. The behavior of sound rays is assumed to be equivalent to ray optics. In the following paragraphs we describe the propagation effects that we model in our simulation.

3.3.1. Reflection

When a sound beam encounters an interface of two tissues with different acoustic impedances, part of its energy is reflected. In the case of specular reflections, if the direction of travel of the beam is perpendicular to the interface, then the beam will be reflected back to the transducer and therefore, a strong echo signal is detected. However, in most of the cases the beam is reflected away from the transducer and only small or no echoes can be detected. If the reflecting surface is rough, as most of the tissue surfaces in the body, diffuse reflections occur. These are predominant in B-Mode scans and therefore we focus on modeling them. In this case, the sound beam is scattered following Lambert's law of cosines, which states that the observed light intensity, or in our case, detected echo strength, is proportional to the angle between the observer's line of sight and the normal of the surface. From this, we calculate the reflected intensity I_r by:

$$I_r = I_i R \frac{\cos \alpha}{\pi d^2} \tag{1}$$

where I_i is the incoming intensity, α is the angle between the incoming ray and the interface normal, d is the distance from the observation point to the interface and R is the reflection coefficient obtained by the well-known formula for intensity reflection:

$$R = \left(\frac{Z_2 - Z_1}{Z_2 + Z_1} \right)^2 \tag{2}$$

where Z_1 and Z_2 are the acoustic impedances of the current and next medium, respectively.

3.3.2. Transmission

The part of the beam's energy that is not reflected $(I_i - R)$ is transmitted farther into the tissue. This gives the next formula for the amount of energy transmitted I_t:

$$I_t = I_i \left(\frac{4 \cdot Z_2 \cdot Z_1}{Z_2 + Z_1} \right)^2 \tag{3}$$

When the encountered interface is highly reflective, i.e., the difference in the acoustic impedance of both materials is large, the transmitted energy is significantly reduced, causing acoustic shadows. Typically, these shadows can be seen behind bones and air-filled structures such as the lungs.

3.3.3. Absorption and Enhancement

As the ultrasound beam travels through tissue, part of its energy is absorbed. The amount of energy that is absorbed depends on the distance traveled and the frequency of the US wave. The formula for calculating the output intensity I_a due to absorption of ultrasound is:

$$I_a = I_i \cdot 10^{-\alpha d f / 20} \tag{4}$$

where α is the absorption coefficient of the medium in decibels dB, d is the distance traveled in the tissue and f is the frequency of the ultrasound wave.

Ultrasound machines compensate the absorption effect by enhancing the incoming echoes based on the traveled distance. Due to this compensation, some structures behind low-absorbing materials, i.e., blood vessels and cysts, can appear brighter than their surroundings.

3.3.4. Scattering

Most of the echo signals received are produced from scattering of the sound within the tissue. Scattering of sound is produced by small particles with different density from the tissue that surrounds them. These scatterers vary in size and are assumed to be distributed uniformly within the tissue. In [IH90], the frequency-dependent backscattering from a spherical particle of diameter D is modeled with:

$$F(f, D) = \left(j_0 \left(\frac{2 \pi f D}{c} \right) \right)^2 \tag{5}$$

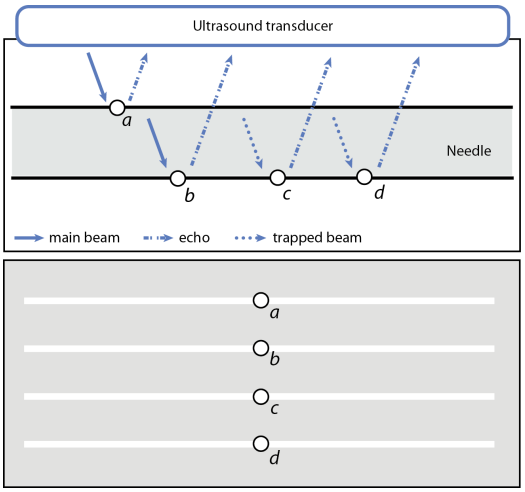

Figure 1: *Reverberation.* Top*, the ray is reflected at point* a *to produce the first echo. The transmitted energy is reflected again at* b*, then at* c *and* d. Bottom*, the resulting structure detected in the process.*

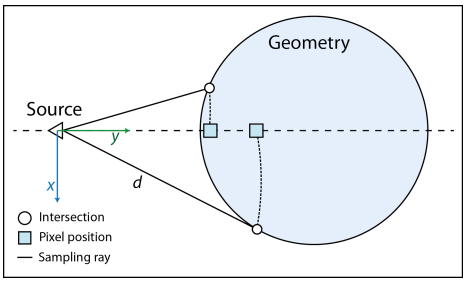

Figure 2: *Pixel sampling and drawing. The pixel is drawn at distance d, determined by the ray length, along the x position of the transducer, marked by the dashed line.*

where f is the US frequency and j_0 is the spherical Bessel function of the first kind, zero order. For more information on Bessel functions we refer the reader to [MI86].

From [IH90] we obtain the following equation to estimate the received backscattered energy σ from a determined volume space with n_t scatterers with different diameters:

$$\sigma = I_i C f^4 \gamma_0 \sum_{k=1}^{n_t} \left[D_k^6 \frac{n_k}{n_t} F(f, D_k) \right] \tag{6}$$

where C is a constant equal to $\left(\pi^4/36c^4\right)$, with c the speed of sound in the medium, f is the ultrasound frequency, n_k is the number of scatterers with diameter D_k, γ_0 is the scattering strength obtained by:

$$\gamma_0 = 4 \left(\frac{Z_1 - Z_2}{Z_1} \right)^2 \tag{7}$$

and F is the backscattering coefficient from an individual scatterer defined above (equation 5).

3.3.5. Reverberation

Reverberation artifacts can occur when a sound beam is *trapped* between two strongly reflecting interfaces, e.g., the walls of a needle. When the sound beam encounters a strong reflector, part of the energy is reflected to produce the original echo. The rest of the energy is transmitted, when it reaches the second interface it is again reflected, in the way back, it is reflected once again by the first interface, then a third time by the second one. And so on until the energy is dissipated. In each reflection, part of the energy penetrates the interface while the other part remains trapped. Eventually, some of the energy from each reflection will reach the receptor, but since the echoes have traveled longer distances, the respective signals are interpreted as if coming from locations deeper in the tissue. Figure 1 describes this behavior. Mirroring artifacts and the so-called comet tails are created in a similar fashion, the difference being the distance between the reflecting layers.

4. Implementation Details

In this section, we will describe in detail how we implement the effects described above.

4.1. Scattering Texture

Equation (6) for the calculation of the backscattering coefficient σ mostly depends on variables that are known before the simulation starts. The only part that must be calculated online, since it depends on the properties of the sampled tissue, is the backscattering strength γ_0. The rest of the formula is pre-calculated and stored in a 3D texture. During simulation, the scattering strength can be calculated only after the acoustic impedance of the medium is obtained, and is then multiplied by the backscattering coefficient from the texture. Both values are obtained depending on the position of the sampled point.

4.2. Image Creation

As described before in 3.1, an US probe is typically composed of an array of transducers that progressively send sound pulses into the tissue and detect the reflected echoes to build an image based on their intensity. To simulate the process, we model a row of transducers that act as the "light sources" in the ray traced scene. For each transducer a number of rays with different directions are sent into the scene. The ray directions are determined by a probability density function described by the beam profile model (section 4.3). Samples are taken at the intersections with objects in the scene or in empty space at regular intervals. In empty space,

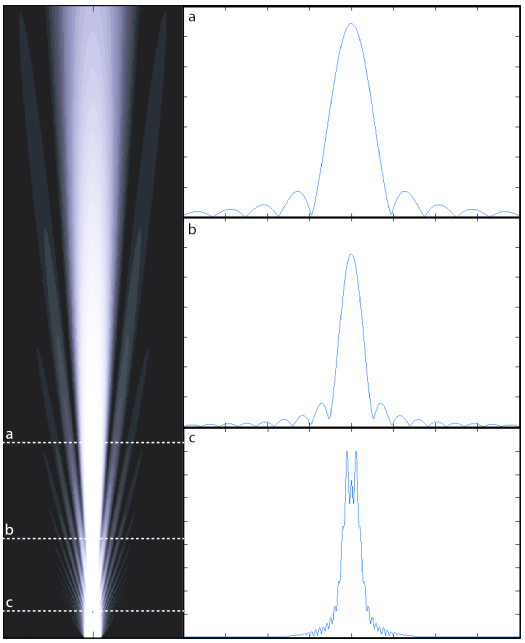

Figure 3: *Beam profile and different probability density functions according to distance from transducer. The dotted lines show approximate positions of the selected pdfs.*

where no intersection is found, a sample from the scattering texture is obtained. At intersections, a number of things happen:

1. The reflected energy of the ray is calculated based on the properties of the tissues involved in the interface and the surface normal (eq. 1).
2. The ray's transmitted energy is calculated (eq. 3).
3. If the reflected energy is high (above a certain predefined threshold), a secondary reflection ray is created to simulate reverberation effects.
4. The intensity of the pixel at traveled distance d is calculated.
5. If the ray's intensity has reached a minimum threshold, the ray is terminated, otherwise, it continues in the same direction with the estimated transmitted energy.

Figure 2 shows a schematic of the sampling procedure. Note that since we use only the distance traveled to determine where to locate the estimated reflected intensities along the transducer's axis, their actual position may not always coincide with the intersection point. The same occurs when sampling the scattering texture. This imitates the behavior described in section 3.1. Additionally, as sound velocity is assumed to be always $1540 m/s$, using distance or time gives the same results. By employing this technique we are able to simulate point spreading and blurring effects, which rise from the fact that the US beam cannot perfectly focus on one spot.

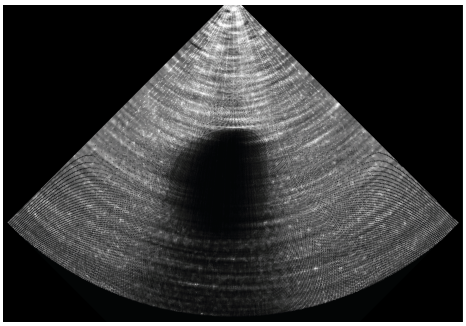

Figure 4: *Curvilinear configuration of transducer array. The proposed model allows simulation of different array configurations.*

4.3. Beam Profile Estimation and Ray Creation

For the estimation of the beam profile model described in section 3.2, we use a superposition of Gaussian beams [WB88]. This is then used as a probability density function (pdf) to determine the direction of sampling rays into the scene, thereby obtaining more samples where the beam intensity is higher, to achieve effects such as point spreading due to the beam focusing and ghosting generated by side and grating lobes. Figure 3 shows the beam profile of a $3.5 MHz$ unfocused circular transducer with radius $6.35 mm$ calculated with a superposition of 10 Gaussian beams in a homogeneous medium, and a progression of the pdf plotted at different distances from the transducer.

For our implementation, we create several rays in different directions. We perform a metropolis random walk to sample the pdf and use the resulting random numbers as the angle, or rather the cosine of the angle, to rotate the ray away from the beam axis. Rays are mirrored to avoid having an unsymmetrical beam profile, that might result due to the small number of samples. The initial intensity I_i for the estimation of reflected and transmitted energies can be changed to simulate gain adjustment. The calculation of each pixel row is performed in a separate thread in the GPU and the final image is a simple union of the rows, i.e., no further addition or calculations are required.

4.4. Geometries and Materials

Body structures, e.g., organs and bones, are modeled with surface representations, i.e., triangle meshes that are stored as a 1-dimensional texture for access by the GPU. Each type of structure has an associated acoustic impedance and absorption coefficient that are used for the different estimations. These values are also stored in a 1-dimensional texture in the GPU and accessed whenever the ray hits an intersection.

5. Results

Using the proposed approach, we are able to simulate a wide range of effects and ultrasound artifacts. For example, by applying small changes to the acoustic impedances we can control the intensity of the reflections and increase the shadowing effects. The model allows varying frequency and focal length to increase or decrease the contrast, brightness and sharpness of the simulated images to imitate the functionality of real US devices. Additionally, we are able to simulate various transducer sizes and array configurations, e.g., rectilinear and curvilinear, by varying the orientation, position and number of virtual transducers. Figure 4 shows a simulated image with a curvilinear array configuration, all other simulated images presented in this paper use a rectilinear configuration. The model is also easily extensible to include additional artifacts, e.g., twin images caused by ray refraction, and common image distortions due to variations of the speed of sound.

5.1. Performance

Currently, the code is not optimized to properly evaluate performance, for example, a naive implementation of a bounding volume hierarchy (BVH) is used to test for intersections of rays and primitives. Preliminary tests, however, show that interactive frame rates can be achieved in some cases. Table 5.1 shows some of the results of these tests.

# of primitives	# of rays per transducer		
	10	30	60
5120	20	10	6
21864	5	3	<2

Table 1: *Some preliminary performance tests results. Approximate frame rates are shown for different number of primitives and rays created per transducer.*

Figure 5 shows three simulated images with different number of rays per transducer. All other images were simulated using 60 rays.

5.2. Validation

For an initial validation of our model and the resulting simulated images, we consulted two ultrasound-guided-regional-anesthesia (UGRA) experts with more than 10 years of accumulated experience, via a review in which we showed sets of images with different artifacts, effects, textures and resolutions. Our goal was two-fold: (1) validate the realism of the produced images and thereby the model itself, and (2) verify the property values found in literature and fine tune them for the simulation. Consequently, we divided the review into 2 parts. Part one consisted of a fine tuning step and in part two, the realism of the fine tuned images was evaluated.

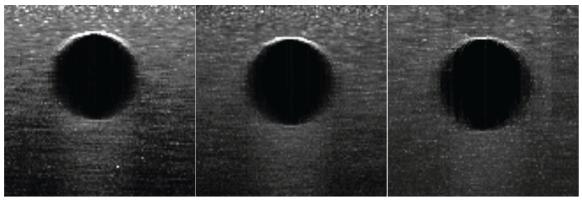

Figure 5: *Simulation with varying number of rays per transducer. From left to right: 60, 30 and 10 rays.*

5.2.1. Fine Tuning of Simulation Parameters

Due to the amount of simulation properties that can be adjusted, the resulting amount of possible scenarios and combinations was too large to evaluate. We decided to limit the sample size and chose, based on observation of real images, the combinations that we considered looked the most realistic. Nevertheless, some possibilities were still left out of the test, e.g., the effects of the variations in frequency and focal length of the beam on the realism of the images was not tested, since this parameters can be adjusted also in real machines.

In total, we used 12 different sets, each set containing different number of images (5-8) depending on the effects and properties we wanted to evaluate. Every image of each set had to be evaluated using a Likert-scale from 1 to 5, with 5 being the highest value meaning the evaluated effect looked totally realistic. The first 5 sets showed images with different texture resolutions and transducer count. The first set of the group contained only noise, the other 4 contained various structures, i.e., bone (fig 6 a), vein (fig 6 b) and needle in plane (fig. 6 c) and out-of-plane(fig. 6 d). For the other 7 sets, we fixed the noise texture and showed the structures and their corresponding artifacts using slightly different material properties for fine tuning. Here we evaluated: a blood vessel with its corresponding enhancement artifact and with and without lateral shadowing, a bone with reflections and shadows, and a needle in four different positions and angles with its corresponding reverberation effect. We also randomized the ordering of the images within each set and used latin squares method among similar sets. During the evaluation, experts were encouraged to comment and ask freely and to give suggestions for improvements on the different images. We also asked the experts to comment on specific assigned values, for example, why was a lower score assigned to an image that looked, in our opinion, very similar to another one with a high rating. The test was applied individually.

5.2.2. Assessing Realism

For the second part of the test, we followed the same methodology, namely, we showed sets of images with slightly different properties that were to be rated with a five value Likert-scale. In this case, we created scenes with combined structures, i.e., veins, arteries, muscle and fascia lay-

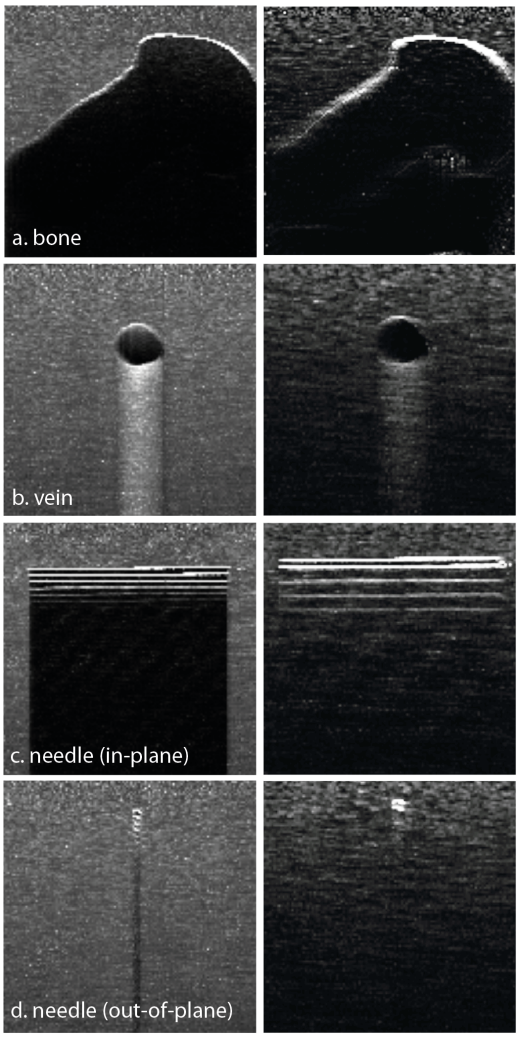

Figure 6: *Ultrasound simulated images. Images in the* Left column *show some of the best rated images during the test; the image to the* Right *show improvements based on the feedback obtained. Improvements were made by adjusting the simulation parameters. Contrast and brightness were manually enhanced for printing.*

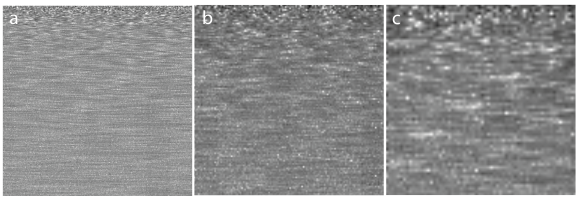

Figure 7: *Textures and resolutions. a)* 512 *transducers with a* 256^3 *texture; b)* 128 *transducers with a* 128^3 *texture; and c)* 64 *transducers with a* 64^3 *texture.*

ers to imitate scenes observed in real US images. Real ultrasound images, Figure 8, were also included in this test, some of which were altered to improve contrast and reduce blurriness. This was not known by the experts.

5.3. Evaluation Results and Discussion

During the fine-tuning step, both experts agreed that the presented images, although plausible, looked too sharp and had too high contrast, as if a very well calibrated machine were used with a homogeneous phantom. Both of these issues could be easily corrected by adjusting the focal length and frequency of the beam, and reducing the resolution of the image. Images in Figure 7 present the same structures using different beam parameters and transducer count. The lowest transducer count used in the test was 128 with a scattering texture of 128^3 texels, which can be easily reduced to produce blurrier images with less homogeneous noise textures.

Using the feedback obtained, we adjusted the parameters to achieve a more realistic simulation and prepare the images for the second part of the review. Figure 6 shows some samples of the simulated images. The column to the left shows some of the images that were rated as the best by the experts during the fine-tuning. The images to the right show the improved images after applying the suggested adjustments.

In the second part of the evaluation, as expected, the real images were all rated as realistic (5 points), even the enhanced ones. Most of the simulated images were also rated as very realistic to realistic (4-5 points). Figure 8 shows a simulated image used in the evaluation that was highly rated by the experts.

One aspect of the simulation that could not be significantly improved by adjusting the parameters, was the reflection of the needle, and consequently the reverberation artifact. As we chose only to model diffuse surfaces and the needle is actually a specular reflector, incorrect reflections for some needle angles are produced. The issue, however, will be solved by adding a new material property to differentiate between diffuse and specular reflectors, thus effectively modeling both types of surfaces.

6. Conclusion and Future Work

We have presented a generative approach for the simulation of B-mode ultrasonic images. The proposed model takes into consideration the properties and behavior of real ultrasound devices and beams traversing through tissue to produce realistic images that can be used for training of ultrasound guided procedures. Furthermore, the flexibility of the approach allows the creation of a diversity of training scenarios, addressing a common issue when training with real patients. It is also possible to change the configuration and number of virtual transducers to simulate different devices and produce, for example, rectilinear and curvilinear images.

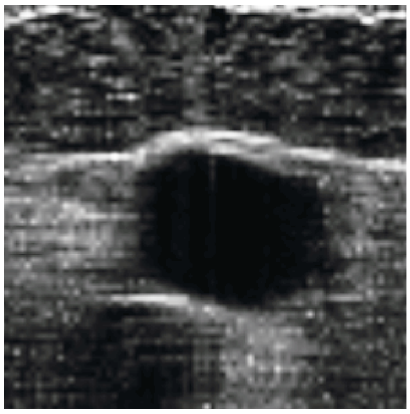

Figure 8: *Simulated scene with vein, artery and other structures.*

Although the initial results are very positive, there are still some improvements needed, namely, specular reflections for the needle should be added. Further validation of the model should also be performed through a user study with a larger group of experts to allow for statistical analysis. Additionally, the model can be also extended to consider refraction of the beam and variation of the sound speed through different tissue. These issues will be addressed in next iterations. Finally, code optimizations will be made to improve overall execution time and more accurate performance tests will be performed.

Acknowledgements

We thank our medical partners at the Department of Anesthesiology at the University Hospital Aachen, for their cooperation in this project. Additionally, the first author of the paper receives a scholarship for his studies from the German Academic Exchange Service (DAAD).

References

[ACO98] AIGER D., COHEN-OR D.: Real-time ultrasound imaging simulation. *Real-Time Imaging 4*, 4 (1998), 263 – 274. 2

[BD80] BAMBER J. C., DICKINSON R. J.: Ultrasonic B-scanning: a computer simulation. *Physics in medicine and biology 25*, 3 (May 1980), 463–79. 2

[GS09] GOKSEL O., SALCUDEAN S. E.: B-mode ultrasound image simulation in deformable 3-D medium. *IEEE transactions on medical imaging 28*, 11 (Nov. 2009), 1657–69. 2

[IH90] INSANA M. F., HALL T. J.: Parametric ultrasound imaging from backscatter coefficient measurements: Image formation and interpretation. *Ultrasonic Imaging 12*, 4 (1990), 245 – 267. 3, 4

[Jen91] JENSEN J. A.: A model for the propagation and scattering of ultrasound in tissue. *The Journal of the Acoustical Society of America 89*, 1 (1991), 182–190. 2

[KSN09] KUTTER O., SHAMS R., NAVAB N.: Visualization and GPU-accelerated simulation of medical ultrasound from CT images. *Computer methods and programs in biomedicine 94*, 3 (June 2009), 250–66. 2

[KWN10] KARAMALIS A., WEIN W., NAVAB N.: Fast ultrasound image simulation using the Westervelt equation. *Medical image computing and computer-assisted intervention (MICCAI) 13*, Pt 1 (Jan. 2010), 243–50. 2

[LN82] LINZER M., NORTON S. J.: Ultrasonic tissue characterization. *Annual Review of Biophysics and Bioengineering 11*, 1 (1982), 303–329. 2

[MI86] MORSE P., INGARD K.: *Theoretical acoustics*. Princeton University Press, 1986. 4

[MZR*07] MAGEE D., ZHU Y., RATNALINGAM R., GARDNER P., KESSEL D.: An augmented reality simulator for ultrasound guided needle placement training. *Medical and Biological Engineering and Computing 45* (2007), 957–967. 10.1007/s11517-007-0231-9. 2

[NCQ*11] NI D., CHAN W. Y., QIN J., CHUI Y.-P., QU I., HO S. S. M., HENG P.-A.: A Virtual Reality Simulator for Ultrasound-Guided Biopsy Training. *IEEE Computer Graphics and Applications 31*, 2 (Mar. 2011), 36–48. 2

[RPAS09] REICHL T., PASSENGER J., ACOSTA O., SALVADO O.: Ultrasound goes GPU: real-time simulation using CUDA. *Proceedings of SPIE* (2009), 726116–726116–10. 2

[SHN08] SHAMS R., HARTLEY R., NAVAB N.: Real-time simulation of medical ultrasound from CT images. *Medical image computing and computer-assisted intervention (MICCAI) 11*, Pt 2 (Jan. 2008), 734–41. 2

[Thi03] THIJSSEN: Ultrasonic speckle formation, analysis and processing applied to tissue characterization. *Pattern Recognition Letters 24*, 4-5 (2003), 659 – 675. 2

[Vor08] VORLÄNDER M.: *Auralization: fundamentals of acoustics, modelling, simulation, algorithms and acoustic virtual reality*. RWTHedition (Berlin. Print). Springer, 2008. 2, 3

[WB88] WEN J. J., BREAZEALE M. A.: A diffraction beam field expressed as the superposition of gaussian beams. *The Journal of the Acoustical Society of America 83*, 5 (1988), 1752–1756. 3, 5

[WBK*08] WEIN W., BRUNKE S., KHAMENE A., CALLSTROM M. R., NAVAB N.: Automatic CT-ultrasound registration for diagnostic imaging and image-guided intervention. *Medical image analysis 12*, 5 (Oct. 2008), 577–85. 2

[Zhu06] ZHU Y.: A virtual ultrasound imaging system for the simulation of ultrasound-guided needle insertion procedures. *Image Rochester NY* (2006), 61–65. 2